A 2D MACRO-ELEMENT FOR EFFICIENT NONLINEAR ANALYSIS OF PILE FOUNDATIONS UNDER SEISMIC LOADING

Thomas Lhermitte, Florent Prunier, David Bertrand, Stéphane Grange, Pierre Wyniecki, Evan Monroig, Thomas Jochyms

COMPDYN 2023
9th ECCOMAS Thematic Conference on
Computational Methods in Structural Dynamics and Earthquake Engineering
M. Papadrakakis, M. Fragiadakis (eds.)
Athens, Greece, 12-–14 June 2023

A 2D MACRO-ELEMENT FOR EFFICIENT NONLINEAR ANALYSIS OF PILE FOUNDATIONS UNDER SEISMIC LOADING

Thomas Lhermitte[1,2], Florent Prunier[1], David Bertrand[1], Stéphane Grange[1], Pierre Wyniecki[2], Evan Monroig[2], and Thomas Jochyms[3]

[1]Univ Lyon, INSA Lyon, GEOMAS, EA7495
69621 Villeurbanne, France
e-mail: {thomas.lhermitte, florent.prunier, david.bertrand, stephane.grange}@insa-lyon.fr

[2] STABILIS
01210 Ferney-Voltaire, France
e-mail: {pierre.wyniecki,evan.monroig}@stabilis.fr

[3] VINCI Construction Grands Projets
92000 Nanterre, France
e-mail: thomas.jochyms@vinci-construction.fr

Keywords: Macro-element, Pile foundation, Earthquake Engineering, Two-phase model, Interface law.

Abstract. *The nonlinear behaviour of pile group foundations subjected to earthquake loading involves several varied phenomena such as soil-pile interaction, pile-raft interaction, soil nonlinearities and pile damaging. To accurately account for these phenomena, a significant number of degrees of freedom are required, especially close to the contact zone between the pile and the soil. This research proposes a novel two-phase model formulated within the framework of a macroelement to take into account the soil-pile interaction. The proposed macro-element uses a multi-scale substructuring approach based on FEM. Each macro-element represents a single-pile and its immediately surrounding soil. The macro-element is an assembly of two-phase elements based on two independent meshes for the pile and for the soil. Interface forces between the pile and the soil are integrated continuously on the interface length with an ad hoc interface constitutive model. The focus of the paper is the presentation of 1D and 2D two-phase elements. Test cases with both linear and nonlinear interface laws are shown to validate the elements.*

1 INTRODUCTION

Use of pile foundations for the construction of large-scale projects on medium quality soils is inevitable. Their earthquake design involves different scales and relates to both structural and geotechnical engineering. Moreover, pile foundations induce a strong coupling of superstructure and foundation behaviour. Both the multi-scale aspect, and the coupling between superstructure and foundation behaviour, make global models difficult to implement, and very time consuming. Thus, the use of macro-element tools appears strongly appealing for modelling soil-structure interaction, in particular for earthquake applications.

The idea of the finite macro-element is to condense the whole {near-field soil + pile + foundation} system response at the foundation center ; the system response is thus formulated as a constitutive force-displacement law in generalized variables.

A number of macro-elements for pile foundations have been developed over the last decade. Among these, an elasto-plastic macro-element was introduced by Correia [1] for bridge monopiles. It takes into account soil plastification and slip between soil and pile. Li and co-workers introduced the first hypo-plastic macro-element for pile foundations [2]. It models in particular the degradation of soil properties with cyclic loading. It was extended by Pérez-Herreros [3] to dynamic pile-group effects.

The present work falls within the framework of the development of a macro-element (2D for the time being) for pile foundations under seismic loading. The macro-element is different from regular macro-elements because it uses a multi-scale substructuring approach based on finite element modelling. It can be considered as an alternate modeling technique at the crossroads between regular macro-element modeling and direct FEM approach. The macro-element represents a single-pile and its immediately surrounding soil. An internal Newton-Raphson procedure solves the nonlinear equations governing the macro-element equilibrium. The computed forces are dynamically condensed [4] on the external nodes of each macro-element for the computation of the global {soil + foundation + structure} response.

This paper focuses on one of the constituents of the macro-element, namely the modelling of the interaction between the pile and its surrounding soil. The nonlinear behaviour of the interaction is described at the interface scale through an ad hoc phenomenological law.

Firstly, new finite elements, taking into account interface forces between soil and pile, are introduced. Secondly, test cases for the validation of these elements are presented and discussed.

2 METHODS

2.1 Two-phase element-modelling

This section adresses the modelling of the nonlinear soil-pile interface. A two-phase modelling concept is assumed : the pile and the soil are represented by two distinct phases, supported by their own distinct finite element mesh. The interaction between the pile phase and the soil phase is computed by continuous integration over the interface of a phenomenological law describing the interface force density in function of the relative displacement between phases. In the general case, the interface law governs the coupled vertical and horizontal responses of the interface.

The following paragraph introduces a new two-dimensional two-phase element that includes the continuous integration over the interface length. The two-dimensional two-phase element is supported by two finite elements types, namely a nine-node quadrilateral (QUA9) for the soil phase of the element, and two two-node Euler-Bernoulli beams for the pile phase (see figure 1). The elements account for the behaviour of the soil, the pile and the soil-pile interface. The shape

functions of the supporting elements are used to interpolate the relative displacement between phases.

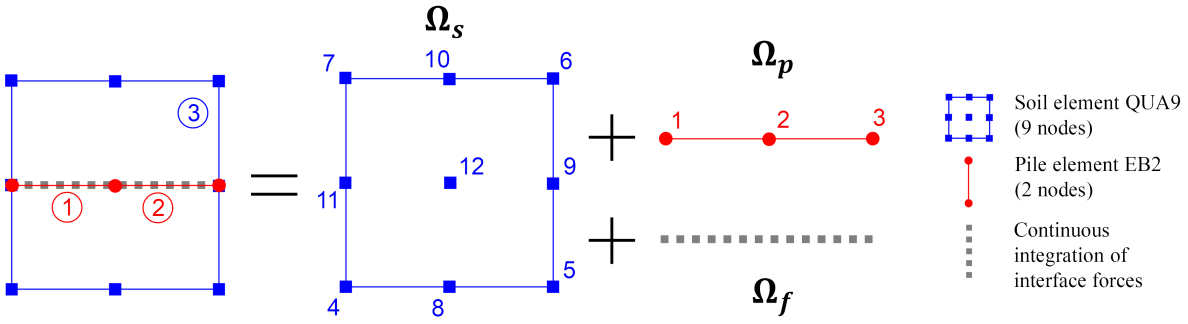

Figure 1: Two-dimensional two-phase element decomposition

Let the Principle of virtual work be applied on an element :

$$\underbrace{\int_{\Omega_{el}} {}^t\boldsymbol{u}^* \rho \ddot{\boldsymbol{u}}\, d\Omega + \int_{\Omega_{el}} {}^t\boldsymbol{\epsilon}^* \boldsymbol{\sigma}\, d\Omega}_{W^*_{int}} = W^*_{ext} \tag{1}$$

where $\boldsymbol{u}$ are the displacements anywhere on the element defined by the domain Ω_{el} and $\boldsymbol{\epsilon}$ and $\boldsymbol{\sigma}$ are respectively the strain and stress tensors rearranged in vectorial form.ρ is the volumic mass. The domain Ω_{el} comprises the pile phase Ω_p and the soil phase Ω_s. The interface is defined as the intersection of both $\Omega_f = \Omega_p \cap \Omega_s$.

The contributions of each of the subdomains to the internal work of the element subjected to the virtual displacement field $\boldsymbol{u}^*$ can be distinguished as follows : a pile contribution $W^*_p = W^*_{pp} + W^*_{pf}$, where W^*_{pf} is the contribution of the soil on the pile at the interface, and a soil contribution $W^*_s = W^*_{ss} + W^*_{sf}$, where W^*_{sf} the contribution of the pile on the soil at the interface.

The contributions W^*_{pp} et W^*_{ss} come from the assembly of the linear mass and stiffness matrices of the two beams and of the quadrilateral of the two-phase element. The contribution of the interface work $W^*_f = W^*_{pf} + W^*_{sf}$ is detailed in the following :

$$\begin{cases} W^*_{pp} = \displaystyle\int_{\Omega_p} {}^t\boldsymbol{u}_p{}^* \rho_p \ddot{\boldsymbol{u}}_p\, d\Omega + \int_{\Omega_p} {}^t\boldsymbol{\epsilon}^*_p \boldsymbol{\sigma}_p\, d\Omega & (2) \\ W^*_{ss} = \displaystyle\int_{\Omega_s} {}^t\boldsymbol{u}_s{}^* \rho_s \ddot{\boldsymbol{u}}_s\, d\Omega + \int_{\Omega_s} {}^t\boldsymbol{\epsilon}^*_s \boldsymbol{\sigma}_s\, d\Omega & (3) \\ W^*_f = \displaystyle\int_{\Omega_f} \left[-{}^t\boldsymbol{u}_{sf}{}^* \boldsymbol{\tau}_s - {}^t\boldsymbol{u}_{pf}{}^* \boldsymbol{\tau}_p \right] d\Omega = \int_{\Omega_f} {}^t\boldsymbol{u}_r{}^* \boldsymbol{\tau}_s \left(\boldsymbol{u}_r\right) d\Omega & (4) \end{cases}$$

where $\boldsymbol{u}_p$ and $\boldsymbol{u}_s$ are the displacements of the pile and the soil in the element, ${}^t\boldsymbol{u}_{sf}$ and ${}^t\boldsymbol{u}_{pf}$ are the displacements evaluated at the interface from $\boldsymbol{u}_p$ and $\boldsymbol{u}_s$. $\boldsymbol{\tau}_p = -\boldsymbol{\tau}_s = -\boldsymbol{\tau}$ is the interface force density which is a function of the relative displacement $\boldsymbol{u}_r = \boldsymbol{u}_{pf} - \boldsymbol{u}_{sf}$ between phases : $\boldsymbol{\tau} = \boldsymbol{\tau}\left(\boldsymbol{u}_r\right)$.

Remark : The Euler-Bernoulli beam assumes plane stresses and the soil quadrilateral plane strains.

Assuming small displacements and strains, and assuming linear behaviour for pile and soil, the contributions W^*_{pp} et W^*_{ss} are expressed classically as :

$$W^*_{ii} = {}^t\boldsymbol{U}_i^{el^*} \left[\int_{\Omega_i} \rho {}^t\mathbb{N}_i\mathbb{N}_i \, d\Omega\right] \ddot{\boldsymbol{U}}_i^{el} + {}^t\boldsymbol{U}_i^{el^*} \left[\int_{\Omega_i} {}^t\mathbb{B}_i\mathbb{C}\mathbb{B}_i \, d\Omega\right] \boldsymbol{U}_i^{el} \ , \quad i \in [p, s] \tag{5}$$

where ${}^t\boldsymbol{U}^{el} = {}^t[\boldsymbol{U}_p^{el}, \boldsymbol{U}_s^{el}]$ are the node displacements of the element and $\boldsymbol{U}_p^{el}$ respectively the pile and $\boldsymbol{U}_s^{el}$ the soil node displacements of the element. $\mathbb{N}_p$ and $\mathbb{N}_s$ are the interpolation functions of the soil and pile elements and $\mathbb{B}_p$ and $\mathbb{B}_s$ their derivatives : $\boldsymbol{u}_p = \mathbb{N}_p\boldsymbol{U}_p^{el}$, $\boldsymbol{u}_s = \mathbb{N}_s\boldsymbol{U}_s^{el}$. Matrix $\mathbb{C}$ contains the material properties, and additionally the cross-section properties in the case of beams.

The interface work W^*_f is integrated over the interface Ω_f. The node displacements at the interface can be written as

$$\boldsymbol{u}_{pf} = \mathbb{N}_{pf}\boldsymbol{U}_p^{el} \tag{6}$$

$$\boldsymbol{u}_{sf} = \mathbb{N}_{sf}\boldsymbol{U}_s^{el} \tag{7}$$

where $\mathbb{N}_{pf}$ and $\mathbb{N}_{sf}$ are the projections of the interpolation functions of the pile and of the soil on the interface (defined by a segment).

Then the virtual relative displacement at the interface can be rewritten as

$${}^t\boldsymbol{u}_r{}^* = {}^t\boldsymbol{u}_{sf}{}^* - {}^t\boldsymbol{u}_{pf}{}^* = \begin{bmatrix} {}^t\boldsymbol{U}_p^{el^*} & {}^t\boldsymbol{U}_s^{el^*} \end{bmatrix} \begin{bmatrix} -{}^t\mathbb{N}_{pf} \\ {}^t\mathbb{N}_{sf} \end{bmatrix} \tag{8}$$

Thus, the interface work can be rewritten as

$$W^*_f = \int_{\Omega_f} \begin{bmatrix} {}^t\boldsymbol{U}_p^{el^*} & {}^t\boldsymbol{U}_s^{el^*} \end{bmatrix} \begin{bmatrix} -{}^t\mathbb{N}_{pf} \\ {}^t\mathbb{N}_{sf} \end{bmatrix} \boldsymbol{\tau} \, d\Omega \tag{9}$$

Interface forces are coupled in vertical and horizontal directions. Simplification of the previous equation by the virtual displacement leads to the elementary effort originating from the interface on the two subdomains of the element.

$$\boldsymbol{p}_f = \begin{bmatrix} \boldsymbol{p}_{pf} \\ \boldsymbol{p}_{sf} \end{bmatrix} = \int_{\Omega_f} \begin{bmatrix} -{}^t\mathbb{N}_{pf} \\ {}^t\mathbb{N}_{sf} \end{bmatrix} \boldsymbol{\tau} \, d\Omega \tag{10}$$

The tangent operator associated to the interface is derived from the latter.

$$\frac{\partial \boldsymbol{p}_f}{\partial \boldsymbol{U}^{el}} = \int_{\Omega_f} \begin{bmatrix} -{}^t\mathbb{N}_{pf} \\ {}^t\mathbb{N}_{sf} \end{bmatrix} \frac{\partial \boldsymbol{\tau}}{\partial \boldsymbol{U}^{el}} \, d\Omega = \int_{\Omega_f} \begin{bmatrix} -{}^t\mathbb{N}_{pf} \\ {}^t\mathbb{N}_{sf} \end{bmatrix} \frac{\partial \boldsymbol{\tau}}{\partial \boldsymbol{u}_r} \begin{bmatrix} -\mathbb{N}_{pf} & \mathbb{N}_{sf} \end{bmatrix} \, d\Omega \tag{11}$$

because

$$\frac{\partial \boldsymbol{\tau}}{\partial \boldsymbol{U}^{el}} = \frac{\partial \boldsymbol{\tau}}{\partial \boldsymbol{u}_r} \frac{\partial \boldsymbol{u}_r}{\partial \boldsymbol{U}^{el}} \tag{12}$$

where $\frac{\partial \boldsymbol{\tau}}{\partial \boldsymbol{u}_r}$ is the tangent operator returned by the interface law.

From a numerical point of view, two integration points are used on each of the beams in the two-phase element, thus amounting to a total of four integration points.

The same strategy can be used to develop other two-phase elements, be they one or three-dimensional. The test case below shows a one-dimensional two-phase element supported by quadratic three-node bars.

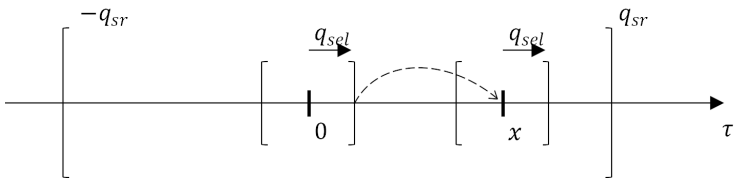

Figure 2: One-dimensional interface law with kinematic hardening

2.2 Interface laws

The interface law expresses the linear density of interface forces as a function of the relative displacement between phases. The law is uncoupled in horizontal and vertical directions for the validation test cases below, but the developed formulation does not preclude the use of a coupled law in the element in a more general case. The same interface law is assumed for horizontal and vertical relative displacements. Two different one-dimensional interface laws are used in the test cases and presented hereafter. The first one is linear elastic :

$$\tau = \pi D k_\tau u_r. \tag{13}$$

where D is the pile diameter, u_r the relative displacement, and k_τ the interface stiffness. This law is used for validation purposes only.

The second law is written within the elastoplastic framework where $du = du^e + du^p$, with du^e and du^p the elastic and plastic relative displacement increments. The law accounts for kinematic hardening. The yield surface f and the hardening rule of the surface are given in the following, distinguishing between a positive and negative trial interface force increment $d\tau_{trial}$:

$$\begin{cases} \text{if } d\tau_{trial} \geq 0 & \\ \qquad f = \tau - (x + q_{sel}) & (14) \\ \qquad x\left(u^p\right) = x_0 + \dfrac{q_{sr} - (q_{sel} + x_0)}{B_p + (u^p - u^{p0})}\left(u^p - u^{p0}\right) & (15) \\ \text{if } d\tau_{trial} < 0 & \\ \qquad f = -\tau + (x + q_{sel}) & (16) \\ \qquad x\left(u^p\right) = x_0 - \dfrac{q_{sr} - (q_{sel} + x_0)}{B_p + (u^p - u^{p0})}\left(u^p - u^{p0}\right) & (17) \end{cases}$$

where x is the moving center of the elastic forces interval, q_{sel} the elastic threshold and as such representing the half-size of the elastic forces interval, q_{sr} the interface force plateau value, x_0 and u^{p0} the values of x and u^p at cycle change (figure 2). B_p is the fitting parameter of the hyperbolic law ; it represents the plastic displacement u^p at $\tau = \frac{q_{sr}}{2} - q_{sel}$ in monotonic loading. If $q_{sel} << q_{sr}$ is assumed, then B_p can be calculated simply from the secant modulus G_{50} at $\frac{q_{sr}}{2}$ following the expression

$$B_p \approx \frac{q_{sr}}{2G_{50}} \tag{18}$$

The flow rule is given by :

$$du^p = d\lambda \frac{\partial f}{\partial \tau} \tag{19}$$

where $d\lambda$ represents the plastic increment.

material	i	$n_i[-]$	$H_i[m]$	$v_i[m.s^{-1}]$	$S_i[m^2]$	$\rho_i[kg.m^{-3}]$	$\eta_i[kg.m.s^{-1}]$	$Z_i[kg.m^{-2}.s^{-1}]$
Air	a	10	200	300	0.04	1.10^{-6}	0	3.10^{-4}
Soft soil	s	20	400	100	0.02	1900	5.10^6	$1,9.10^5$
Pile	p	20	400	582	0.02	2100	2.10^6	$12,2.10^5$
Rock	r	20	1000	500	0.04	1900	0	$9,5.10^5$

Table 1: Properties of soil layers and pile

The elastic displacement increment is calculated as

$$du^e = G^t_{ini} d\tau \tag{20}$$

where G^t_{ini} the initial tangent pseudo-module.

Finally, the tangent modulus of the law is given by

$$G^t = \frac{\frac{\partial f}{\partial x}\frac{\partial x}{\partial u^p} G^t_{ini}}{\frac{\partial f}{\partial x}\frac{\partial x}{\partial u^p} - G^t_{ini}} \tag{21}$$

Only three parameters are involved in this law, namely the elastic threshold q_{sel}, the interface force plateau value q_{sr}, and the secant modulus G_{50} at $\tau = \frac{q_{sr}}{2}$ in monotonic loading.

3 NUMERICAL RESULTS AND DISCUSSION

This section presents two validation test cases. The first one validates a 1D two-phase model composed of two three-node bars under dynamic forces. The second one validates the previously presented 2D two-phase element based on Euler Bernoulli beams and nine-node quadrilateral (QUA9) under static cyclic forces. The main idea in these validation cases is to vary the interface stiffness and compare it to a case where an infinite interface stiffness is defined. The interface behaviour is also tested in a nonlinear case.

3.1 Test case for 1D two-phase element : dynamic loading

A three-layered soil under compression waves is considered. A pile is embedded in the intermediate soil layer. The whole system is modeled by 1D two-phase elements composed of two three-node bars (figure 3). Interface stiffness is only added in the intermediate soil layer. Each bar is defined by its cross-section area S_i, volumic mass ρ_i, Young's modulus E_i calculated from the wave propagation velocity v_i, and internal damping coefficient η_i. All soil layer properties are given in table 1 below, including the impedances $Z_i = \rho_i v_i$, the heights H_i, and the number of bar elements per layer n_i.

Viscous dampers are added at the top and bottom of the model to simulate no-reflection boundaries. Their damping parameter c is chosen so as to cancel out the incoming stress, according to Lysmer and Kuhlemeyer with $a = 1$. The above mentioned linear elastic interface law is used (eq 13). Different interface stiffnesses are tested : $k_\tau = 0$, 2.10^2, 3.10^3, 1.10^4, 1.10^5 and 1.10^8 Pa/m. When the interface stiffness is high, the system is supposed to behave as if the soil and pile phases acted as one layer of equivalent {soil+pile} properties. When the interface stiffness is null, phases should behave independently. The transfer functions between bottom and top of the intermediate layer are calculated analytically on both phases to serve as reference. Assuming an equivalent intermediate soil layer indexed ps, and considering that impedances $Z_{ps} << Z_a$, the transfer function can be expressed as :

$$F(\omega) = \left| \frac{2}{e^{ik^*_{ps}h_{ps}} + e^{-ik^*_{ps}h_{ps}}} \right| \tag{22}$$

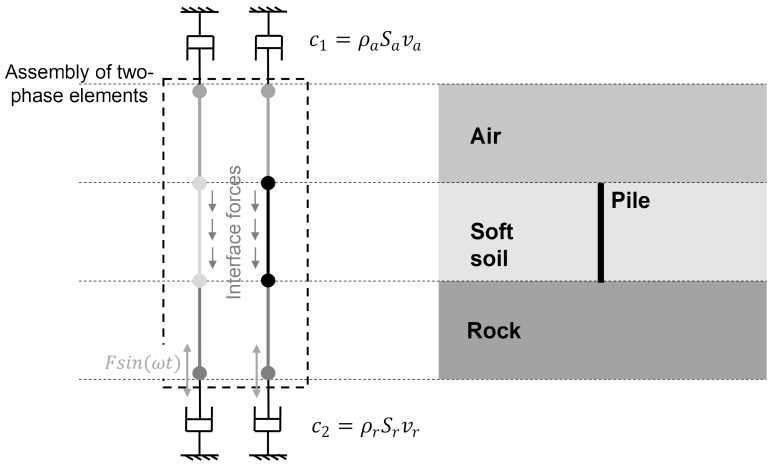

Figure 3: Interface stiffness and boundary conditions of the one-dimensional test case model

where $k^* = \frac{k}{\sqrt{1+\frac{\eta_{ps} i\omega}{\rho_{ps} v_{ps}^2}}}$ and $k = \frac{\omega}{v_{ps}}$ the wave number.

Assuming α and β such that $S_p = \alpha S_{eq}$ and $S_s = \beta S_{eq}$ (here $\alpha = \frac{1}{2}$ and $\beta = \frac{1}{2}$), equivalent properties can be expressed as

$$\begin{cases} \rho_{eq} = \alpha\rho_p + \beta\rho_s & (23) \\ v_{eq} = \sqrt{\dfrac{\alpha\rho_p v_p^2 + \beta\rho_s v_s^2}{\rho_{eq}}} & (24) \\ \eta_{eq} = \alpha\eta_p + \beta\eta_s & (25) \end{cases}$$

Remark : The analytical equilibrium is written with stresses, which explains that the cross-section area needs to be constant between layers. In the intermediate layer, the area is therefore shared between the pile and the soil.

Transfer functions, both analytical and numerical, are presented hereafter firstly for limit interface stiffness values (figure 4) and secondly for intermediate ones (figure 5). Figure 4, shows that the two-phase model matches the reference on the limit cases. When the interface stiffness is very high, the intermediate layer behaves as if phases were glued. As can be observed on figure 5, when the interface stiffness is slightly different from the limit cases, transfer functions also slightly vary from the reference functions. When the interface stiffness varies, resonance frequencies change.

3.2 Test case for 2D two-phase element

3.2.1 Static monotonic loading

The two-dimensional model represents a pile embedded in homogeneous soil. The pile properties are as follows : length $L_p = 13\ m$, cross-section $S_p = 0.5\ m^2$, inertia $I_p = 0.01\ m^4$, circumference $p_p = 2\sqrt{\pi S_p}\ m$ and Young's modulus $E_p = 210.10^9\ Pa$. The soil properties are given hereafter : length $L = 15\ m$, width $H = 10\ m$, Young's modulus $\frac{E_p}{E_s} = 10^2$ (case B) or 10^4 (case A), Poisson's ratio $\nu_s = 0.2$.

Displacements are zero on three boundaries as shown on figure 6a. Static Horizontal unitary displacement is imposed on the pile head. Two models are considered. The reference model

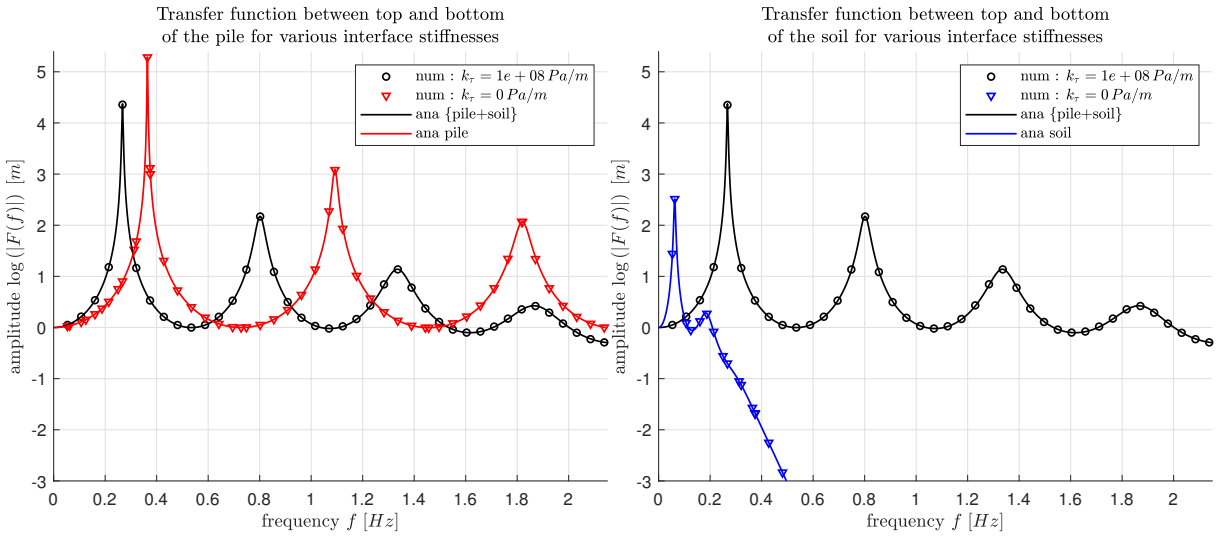

(a) pile (b) soil

Figure 4: Comparison of analytical and numerical transfer functions on the pile (a) and the soil (b) for interface stiffnesses $k_\tau = 0\,Pa/m$ and $k_\tau = 1.10^8\,Pa/m$

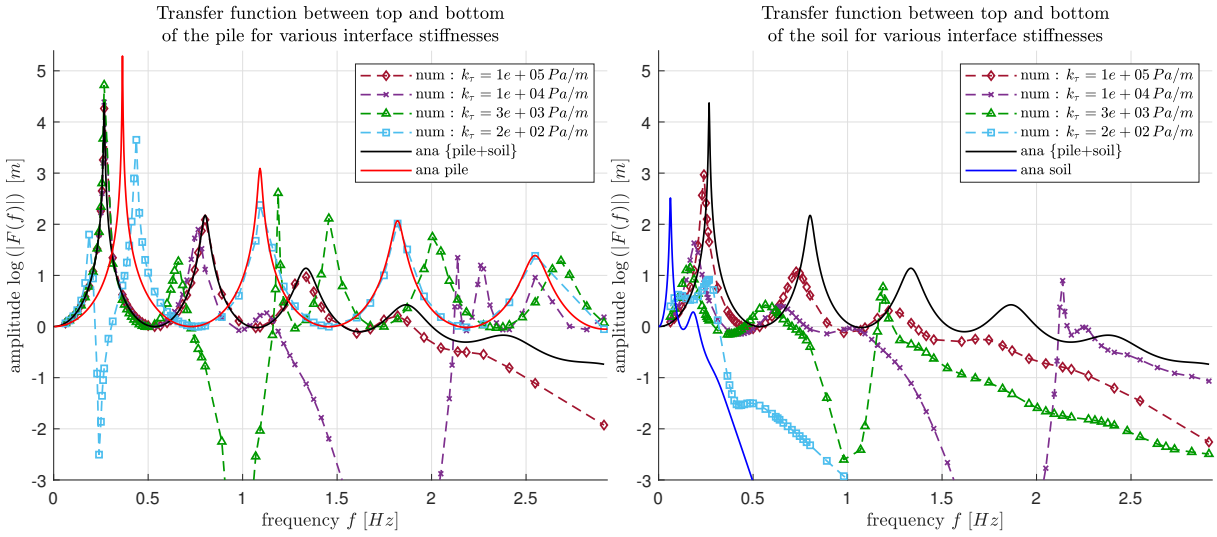

(a) pile (b) soil

Figure 5: Numerical transfer functions for different interface stiffnesses on pile (a) and soil (b)

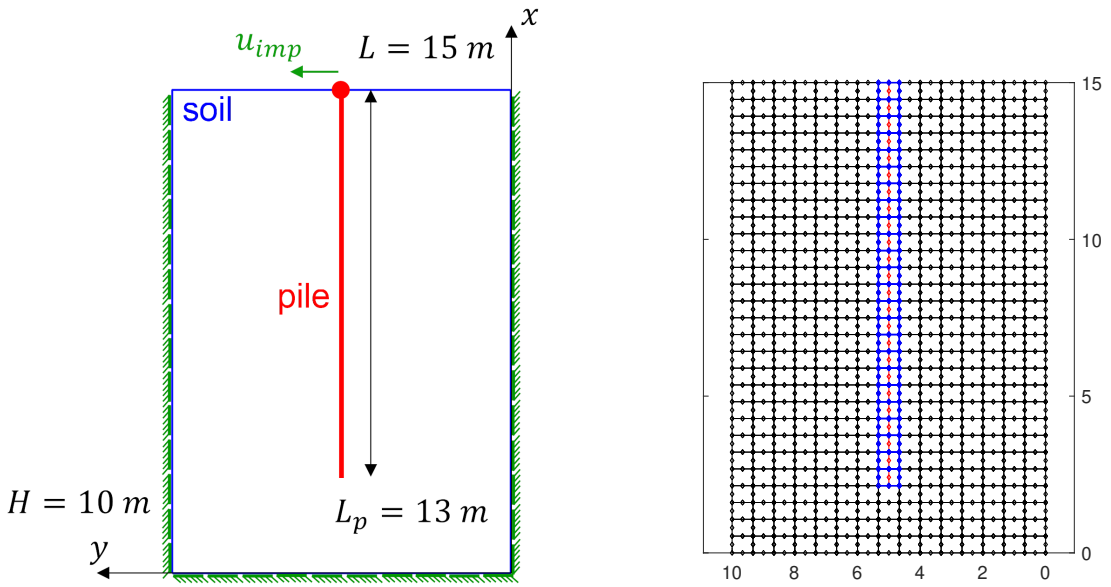

(a) Boundary conditions for the soil box (b) Finite element mesh

Figure 6: Illustration of 2D test case : pile in soil box

$case$	$\frac{E_p}{E_s}$	k_τ
$A1$	10000	$1.00E+08$
$A4$	10000	$1.00E+11$
$B1$	100	$1.00E+10$
$B4$	100	$1.00E+13$

Table 2: Model properties for 2D test case in monotonic loading

does not use two-phase elements. Its pile nodes are merged with those of the soil. The two-phase model uses the linear elastic law presented above. Multiple stiffness values are tested to verify that the two-phase model behaviour tends to the reference model's behaviour with increasing interface stiffness.

The following table 3 shows the horizontal displacement at pile foot $U_{p,foot}$ and the horizontal reaction force at pile head $P_{p,head}$ and their relative difference to the reference model (indexed R). Table 3 shows very low relative deviation on target displacement and reaction force between the reference and the two-phase model with high stiffness (cases A4 and B4). A mesh refining study (not presented here) has shown that the elements do converge.

3.2.2 Static cyclic loading

The same model as before is used, except for the interface law and for the loading. Instead of a unitary static displacement, a static cyclic displacement ranging from 0 to $1.5\,m$ is imposed. The cyclic interface law parameters are uniform with pile depth : $q_{sr} = 2.10^9 \frac{Es}{Ep}\,Pa$, $q_{sel} = 10^4 \frac{Es}{Ep}\,Pa$ and $G_{50} = 4.10^{10} \frac{Es}{Ep}\,Pa$. Parameters are the same for vertical and horizontal relative displacements, though the horizontal interface only very slightly reacts since its relative displacement is only due to Poisson effect.

The force-displacement curves for both test cases A and B are given in figure 8. They serve

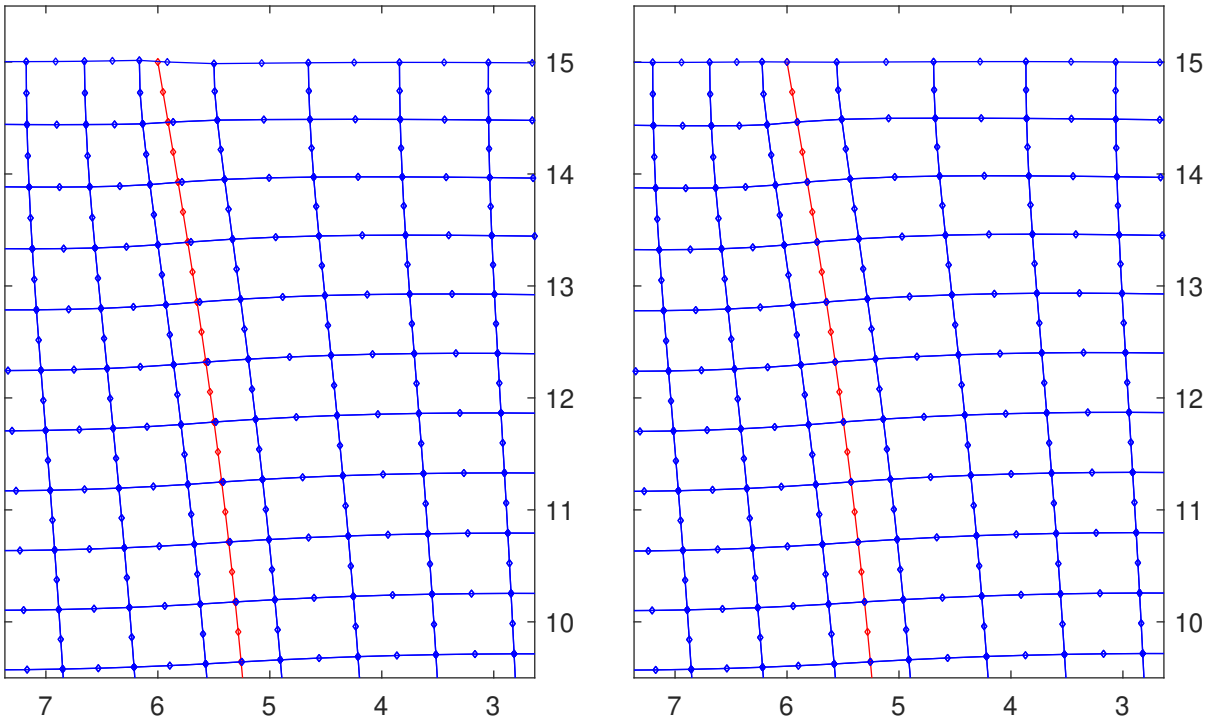

(a) case A1

(b) case A4

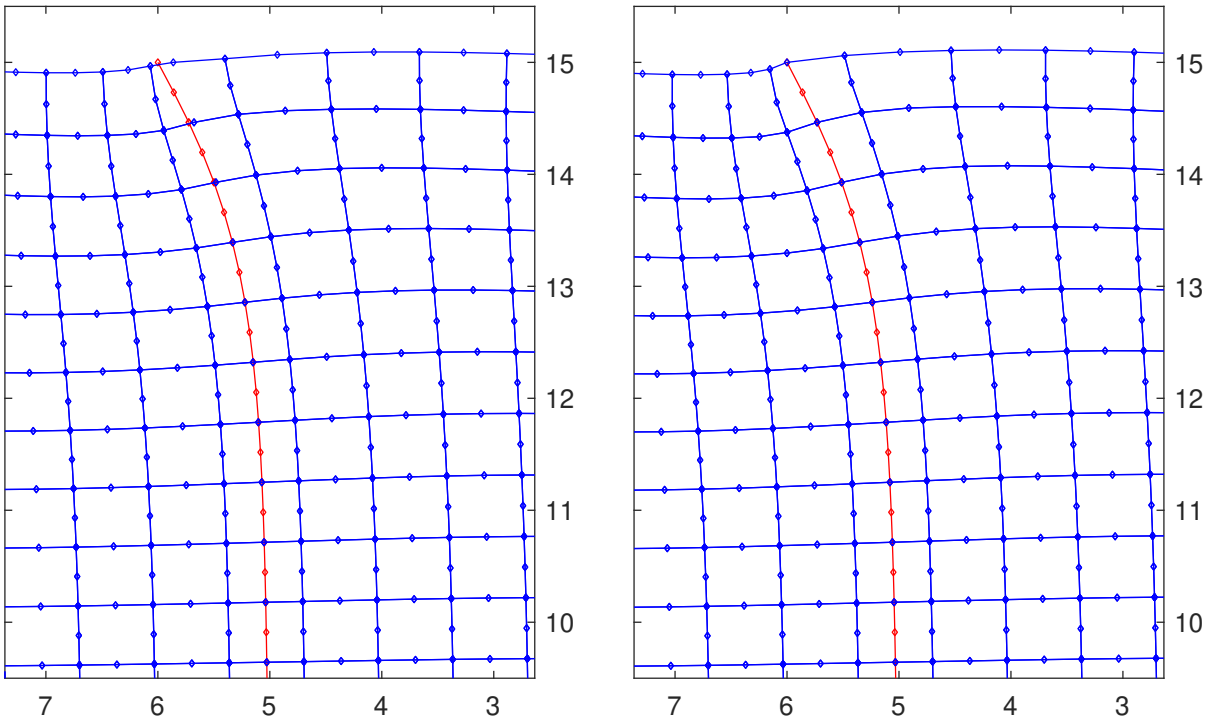

(c) case B1

(d) case B4

Figure 7: Comparison of deformed shape at pile head for 2D two-phase model between cases A1, A4, B1 and B4

$case$	$U_{p,foot}\,[m]$	$P_{p,head}\,[N]$	$\frac{\Delta U_{p,foot}}{U^*_{p,foot}}\,[\%]$	$\frac{\Delta P_{p,head}}{P^*_{p,head}}\,[\%]$
AR	-0.1211	$2.954E+07$		
$A1$	-0.1387	$2.826E+07$	14.59	4.32
$A4$	-0.1211	$2.954E+07$	0.03	0.00
BR	$-3.502E-04$	$1.537E+09$		
$B1$	$-3.779E-04$	$1.407E+09$	7.91	8.44
$B4$	$-3.499E-04$	$1.537E+09$	0.08	0.04

Table 3: Comparison of two-phase element model with reference model (merged nodes) (R) for low stiffness value case A and high stiffness value case B

illustrative purposes, showing nonlinear capabilities of the interface modeling.

4 CONCLUSION

New pile-soil interface finite element modelling has been introduced based on a two-phase approach. Its static and dynamic behaviour has been validated for one- and two-dimensional finite elements. A simple one-dimensional interface law has been introduced for illustrative purposes. Future developments will focus on improving pile-soil interface law in 3D with coupled axial and transverse directions. These improvements are to be included in a 3D macro-element for pile group foundations, which is intended to further model the nonlinear pile-head connection and nonlinear behaviour of reinforced concrete piles. The advantages of such macro-element modelling are the improved ergonomy and numerical convergence properties through a substructuring approach, especially in the case of numerous nonlinearities.

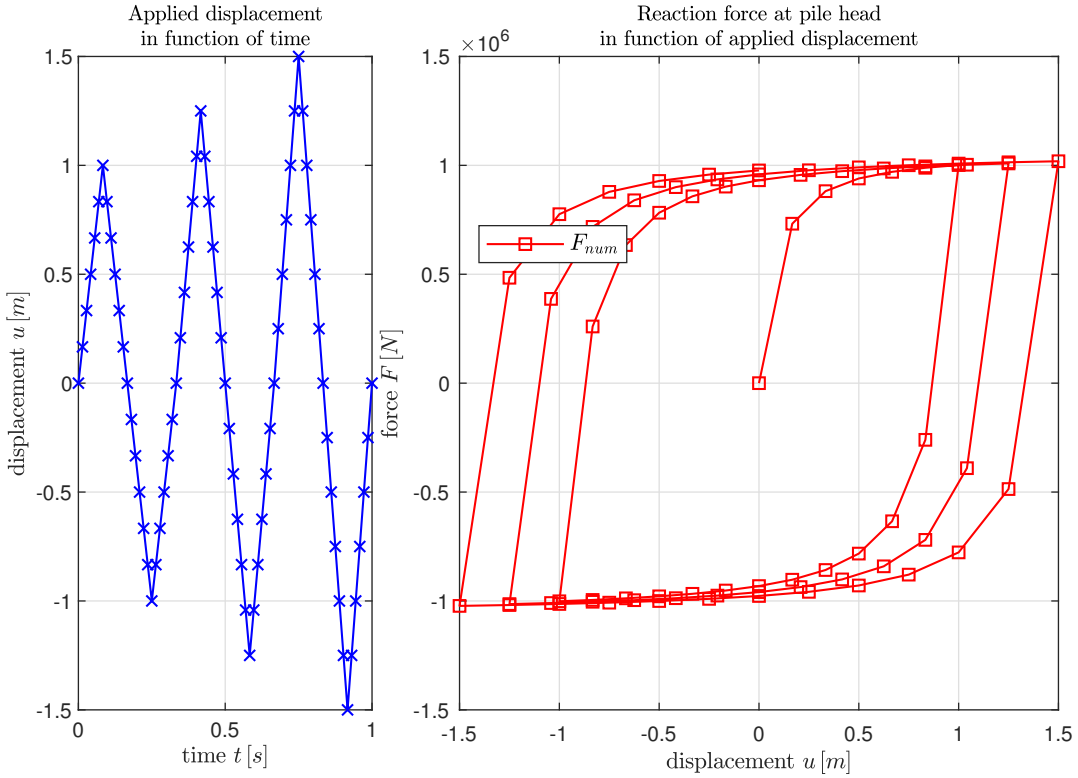

(a) case A

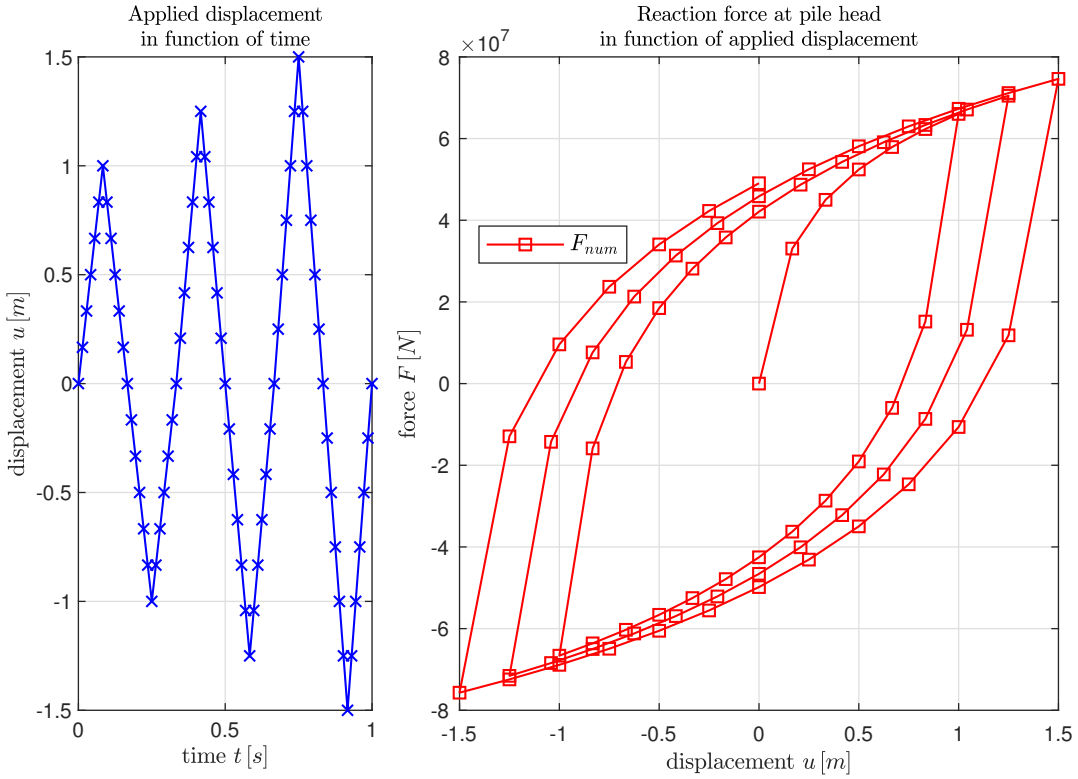

(b) case B

Figure 8: Force-displacement curves at pile head for cyclic loading on cases A and B

REFERENCES

[1] A. A. Correia. *A pile-head macro-element approach to seismic design of monoshaft-supported bridges*. PhD Thesis, Università degli Studi di Pavia, 2011.

[2] Z. Li. *Experimental and numerical study of deep foundations under seismic loading: vertical piles and inclined piles*. PhD Thesis, École centrale de Nantes, January 2014.

[3] J. Pérez-Herreros. *Dynamic soil-structure interaction of pile foundations : experimental and numerical study*. PhD Thesis, École centrale de Nantes, February 2020.

[4] S. Grange and D. Bertrand. Implicit coupling of heterogeneous and asynchronous time-schemes using a primal approach based on velocity continuity at the subdomain interface. *Finite Elements in Analysis and Design*, 196:103604, November 2021.